PalaeoMath 101

Who is Procrustes and What Has He Done With My Data?

To this point in our discussion of geometric morphometrics we've focused mostly on developing background concepts: landmarks, size, shape, shape coordinates. Over the next two essays we'll continue to develop necessary background, but now we'll be discussing concepts fundamental to the current practice of geometric morphometrics and to mathematical shape theory. In the context of this discussion we'll learn why almost everything we've discussed in this entire essay series, while valid in its own right as a set of powerful approaches to generalized data analysis, has been a bit off the mark when it comes to shape analysis. However, we'll resolve this disturbing realization by learning how, with a few relatively minor changes, we can use the same data-analysis approaches to construct a new, very powerful and theoretically consistent approach to the analysis of shape that is ideally suited to tackling the most sophisticated shape-analysis problems we can imagine.

This discussion beings, innocently enough, with a consideration of an alternative metric that can be used to express similarities and differences between the shape of sets of corresponding landmark points. Recall that, in the last essay, we discovered how to use Bookstein's shape coordinate (BSC) approach to transform landmark coordinate data from their raw form — in which size and shape information are complexly confounded — into a mathematical space that uses a landmark-defined baseline to standardize the data for position, size, and rotational differences.

In terms of preserving the geometry of the forms, therein lies the rub. Baseline registration artificially fixes the positions of the baseline landmarks which, in the overwhelming majority of cases, should also be regarded as representing sites of localized shape variance, just like the other landmark positions. There may be some cases in which we have reason to expect that most of the shape variation we're interested in is located in one particular region of the form (see below). Similarly, we may wish to test a hypothesis that focuses its attention on a localized region of the form. In those cases it may seem as though Bookstein shape coordinates would be appropriate. But even in these cases the choice may be questionable. This is because the BSC approach actively *transfers* the shape variance of the baseline landmarks to the other landmarks — variance that wasn't present at those locations to begin with. This transference results in a systematic distortion of the geometry of the BSC space, the intensity and directions of which will vary depending on which landmarks are chosen to define the baseline.

Because of this distortion due to transference of shape variance, there is an additional BSC issue to note. This has to do with the relation between BSCs and centroid size. Recall centroid size is the size index maximally uncorrelated with shape as defined by comparable sets of landmarks. This size index is calculated by summing the squares of distances of all landmark coordinates from their common centroid (= mean). Since the positions of the landmarks in the BSC space have been altered due to the transference of shape variance from baseline to non-baseline landmarks (a transference that has nothing to do with the landmarks' centroid), the value of the size estimate is affected. Even worse, it's affected in a particularly subtle manner.

Since centroid size is calculated using the raw coordinates, the estimate of centroid size itself is not affected by transformation of the raw data into the BSC space, or into any other shape-coordinate space for that matter. However, since superposition is supposed to standardize the landmark configuration for size differences, and since the size standardization implemented by the Bookstein approach is referenced to the baseline (and not the centroid), the size standardization achieved by BSC has, literally, nothing to do with the centroid and so nothing to do with centroid size. This results from the fact that the position of the centroid of the landmark configuration is distorted by transference of shape variance away from the baseline in the same manner as the positions of the non-baseline landmarks. This transference problem also affects the other two aspects of generalized shape coordinate transformation — translation and rotation — in exactly the same way.

Table 1 shows the effect of this discrepancy between baseline size standardization and centroid size standardization for a few of the trilobite pygidium landmark configurations used in the previous essay (see the *Palaeo-Math 101-2* spreadsheet for details of the calculations). Note that, after BSC transformation, the baselines of each configuration are standardized for size (= length), but the centroid size values of the same configurations in the BSC space are not.

Table 1. Lack of precise size standardization for Bookstein shape coordinate superposed data. These are baseline lengths and centroid sizes for trilobite pygidial triangles. See text for discussion and the *Palaeo-Math 101-2* spreadsheet for calculations.

Genus	Baseline Length (Raw Coords)	Centroid Size (Raw Coords)	Baseline Length (BSC)	Centroid Size (BSC)
Acaste	9.244	7.224	1.000	0.781
Balizoma	5.592	4.332	1.000	0.775
Calymene	16.917	12.649	1.000	0.748
Ceraurus	9.796	7.354	1.000	0.751

Mark Webster and David Sheets have developed a partial correction for this BSC shape-variance transfer problem that involves adjusting the length of the Bookstein baseline to bring the size standardization achieved into better conformance with the expectations of a size standardization based on true centroid size. This supplement to BSC transformation has been termed 'sliding baseline registration' (SBR, see Webster *et al.* 2001; also Kim *et al.* 2002). While SBR correction minimizes aspects of the distortions induced by baseline registration, it does not eliminate them. In addition, SBR does not compensate for the effect of arbitrary baseline choice.

So, if Bookstein shape coordinates are a pragmatic and easy-to-understand, but ultimately imperfect means of summarizing shape variation, is there a better approach? Recall that in the last column I mentioned the existence of an alternative shape space. It's now time to introduce you to this alternative shape space — which lies at the very heart of geometric morphometrics and shape theory — in the guise of a figure from Greek mythology.

Procrustes is a character from the legend of Theseus, the founder-hero of Ionia. Theseus met Procrustes on the last leg of his journey from Troezen to Athens. Procrustes was a particularly sadistic bandit who operated in the hills outside Eleusis in southern Greece. A son of Poseidon, Procrustes offered travellers a hospitable break from their journey, plied them with food and drink, and then offered them a bed to rest on. But if the traveller was too long for the bed, Procrustes made them fit by amputating their head and feet. If too short he stretched them with lethal result. Coincidental fits were avoided by Procrustes adjusting the length of the bed after sizing the traveller up from a distance. Being wise to the ways of the world Theseus worked out Procrustes' game beforehand and gave the bandit a taste of his own hospitality, much to the relief of the local inhabitants.

As with the names of many mathematical procedures, the name of this myth's villain has been appropriated as the name of a set of mathematical techniques designed to adjust the scale of datasets while preserving aspects of their internal structure.[1] For example, a hyperbolic rotation (also known as a 'Procrustian stretch) is a mathematical transformation rule used in geometry to convert circles into ellipses of the same area. In generalized data analysis Procrustean methods are used in a wide variety of applications and have a long history. In particular, a number have been developed to rotate the axes of principal components and factor analysis ordinations to positions such that the axes remain orthogonal, but achieve a better alignment with the extreme points in the ordination. This operation is felt by some to improve the stability and interpretability of PCA or FA results.

Morphometrically speaking the landmark alignment methods referred to as Procrustes superposition techniques were first developed in the context of 'theta-rho' (or Θ,ρ) analysis (Benson 1967), which has an interesting palaeontological connection. In seeking to develop a procedure to quantify the structure of shape similarity between species of freshwater ostracodes, palaeontologist Richard Benson hit on the idea of centring a polar coordinate system on some convenient feature of the ostracode carapace (e.g., a muscle scar) and using that to locate the positions of other features (e.g., muscle scars, pore-conuli, carapace outline) using the standard polar coordinate method of describing positions as vectors that lie at an angle (Θ) from a reference line passing through the coordinate system's origin and a radius (ρ)

[1] In their discussion of Procrustes superposition Zelditch *et al.* (2004) offer the interesting observation that Procrustes method of adjusting traveler size was not necessarily Procrustean in a mathematical sense in that the amputation of heads and feet changed the spatial structure of the traveler. Of course, the analogy is with Procrustes' stretching method of traveler adjustment.

from that origin. These Θ,ρ coordinates are completely analogous to the x,y coordinates of the Cartesian system and can be used to represent geometric form in the same manner.

Benson originally used his theta-rho descriptions to represent form differences between ostracode carapace shapes by simply finding the sum of displacements between corresponding landmark points and using those sums to construct a form-distance matrix, the structure of which was represented by a cluster analysis. Later, Benson and colleagues added a technique for comparing forms pioneered by Peter Sneath (1967), who used a two dimensional trend-surface analysis approach to "fit' one set of landmarks to another. The objective of this fitting technique was to (1) maintain the relative configuration of all points in each dataset to one another and (2) minimize the squared distances between corresponding landmarks across the two datasets. Sneath approached this problem as an exercise in two-dimensional curvilinear (or multiple) regression (see MacLeod 2005). But mathematicians and biologists with a mathematical bent quickly realized that there are many possible approaches to this problem (e.g., Mardia and Dryden 1989; Gower and Dijksterhuis 2004).

In geometric morphometrics the term 'Procrustes superposition' usually refers to the variant that is technically known as generalized least-squares (GLS) superposition. As there are other types of superposition procedures (see below) it is best to treat the term 'Procrustes superposition' as a generic or class-level descriptor for the entire family of techniques that minimize differences in position, scale, and rotation for sets of landmark (and/or semilandmark) points. Unfortunately, few authors respect this distinction. I'll illustrate the basic steps in Procrustes (GLS) superposition procedure using the two sets of three pygidial landmarks for the *Calymeme* and *Dalmanities* specimens from the trilobite dataset (Fig. 1).

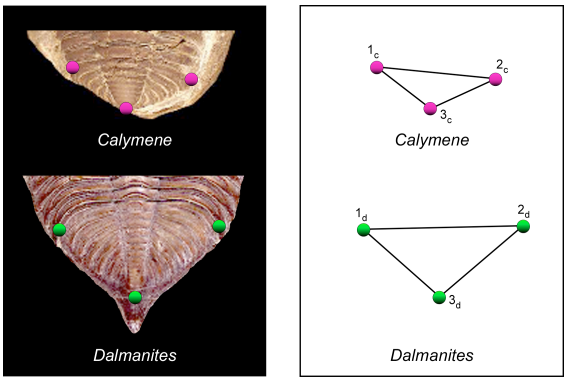

Figure 1. Landmarks used to define triangles that summarize the gross form of *Calymeme* and *Dalmanities* pygidia.

There are two primary methods for calcuating a Procrustes (GLS) superposition, one based on Sneath (1967) and the other developed by Gower (1971). I'm going to base my presentation of the technique on Sneath's approach because it employs simpler mathematics. Readers interested in a full treatment of algorithms and options should consult Rohlf and Slice (1990) or Gower and Dijksterhuis (2004). Remember, what we're after with this operation is a superposition of landmark datasets that aligns their position, their size, and orients them rigidly such that the sum of the squared differences between corresponding landmarks is minimized. Accordingly, it's best to think of the mathematical procedure as involving three discrete steps.

Step 1: Alignment of position (translation)
Obviously the two triangles in Fig. 1 occupy different positions on the page. Therefore, the first step in their superposition is to get them into the same place, one on top of the other. Since we must assume that each landmark represents a localized region of shape variability, it's not appropriate to use any of the landmarks as a basis for this superposition. That being the case we need some other 'fixed point' we can use to achieve standardization via translation.

In the original formulation of theta-rho analysis, Benson used a landmark that represented the location of a homologous feature located in the vicinity of the ostracode carapace's centre as this fixed point. If such a feature—that could be represented by a single point — existed in the set of specimens you were analyzing this might be a reasonable choice, depending on the morphological hypothesis under consideration. However, in our set of trilobite pygidia no such

feature exists. Moreover, from a purely geometric point of view, the selection of a feature unrelated to the geometry of the landmark points themselves will always result in a sub-optimal alignment, at least in a mathematical sense. In most cases the best point to use to achieve standardization via translation is the mean of all landmarks within each dataset, otherwise known as the dataset's centre or centroid. You can use the following simple equations to calculate the x,y coordinates of the centroid of any set of landmark data.

$$\bar{x} = \sum_{i=1}^{m} x_i \Big/ m \ , \ \bar{y} = \sum_{i=1}^{m} y_i \Big/ m \qquad (16.1)$$

In these equations *m* is the number of landmarks in the dataset. Once the centroid has been determined the set of landmarks can be rigidly shifted such that the centroid occupies the origin of a common *x,y* coordinate system by subtracting the mean values of *x* and *y* from each landmark coordinate.

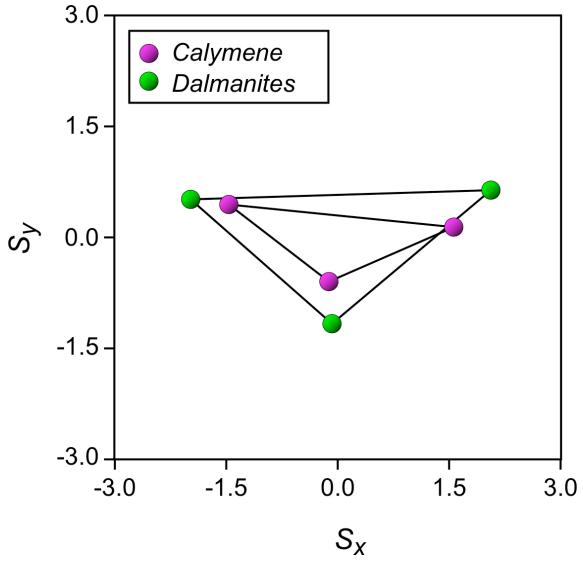

Figure 2. Trilobite pygidial landmark sets after translation via superimposition of their centroids. Note that the centroids of each dataset have been placed at the origin of the coordinate system.

$$\begin{aligned} xtrans_i &= x_i - \bar{x} \\ ytrans_i &= y_i - \bar{y} \end{aligned} \qquad (16.2)$$

When this operation has been completed for the example pygidia data a plot of the translated coordinates will look as follows (Fig. 2).

Step 2: *Alignment of size (scaling)*
The next step involves bringing the two sets of landmarks into alignment by removing the effect of size differences. As we discussed last time, the standard size metric used throughout geometric morphometrics is centroid size. While there are a number of different formulations of centroid size we could use, we're going to adopt the 'industry standard', root centroid size index (*RCS*, see MacLeod 2008).

$$RCS = \sqrt{\sum_{i=1}^{n} \left(x_i - \bar{x}\right)^2 + \left(y_i - \bar{y}\right)^2} \qquad (16.3)$$

Application of this formula to the *Calymene* and *Dalmanites* datasets yields *RCS* values of 2.28 and 3.20 respectively. These values can then be used to rigidly scale each landmark dataset to

a common size, the most convenient of which is the unit value (*RCS* = 1.0). To perform this operation each *x* and *y* coordinate value is divided by the *RCS* value for the landmark configuration as a whole.

$$\begin{aligned} xscaled_i &= xtrans_i / RCS \\ yscaled_i &= ytrans_i / RCS \end{aligned} \tag{16.4}$$

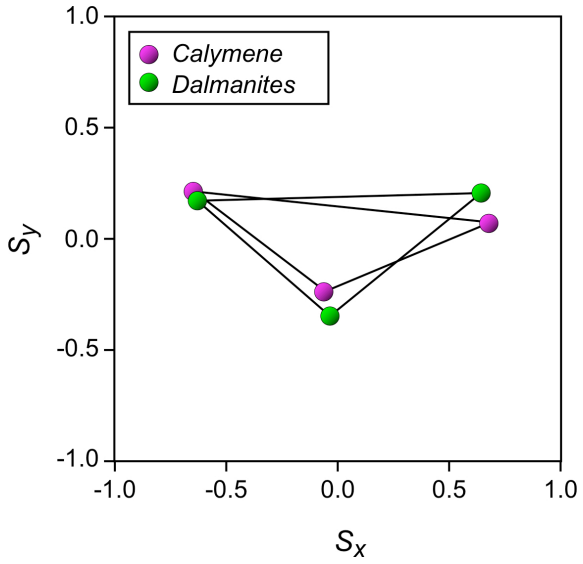

Figure 3. Trilobite pygidial landmark sets after translation via scaling to unit *RCS*. Note the change in the scale of the axes. The shape space is now scaled to *RCS* units.

When this scaling operation has been completed for the example pygidia data a plot of the translated coordinates will look as follows (Fig. 3).

Step 3: *Alignment of orientation (rotation)*
The final step in the Procrustes (GLS) superposition procedure involves rigidly rotating the landmark configurations about their centroids to obtain the best possible fit between corresponding landmark positions. For the initial rotational alignment it's convenient to think of one configuration as the target (*T*) and the other as the configuration that is being rotated (*R*) to an orientation of maximum shape correspondence with respect to the target. For the purposes of our example I'll designate the *Calymene* dataset as the *T* configuration and the *Dalmanites* as the *R*.

Sneath (1967) provides the following equation to calculate the optimal angle through which to rotate the *R* configuration to match the *T*.

$$\theta = \arctan\left(\frac{\sum_{i=1}^{m} y_{Ti}x_{Ri} - x_{Ti}y_{Ri}}{\sum_{i=1}^{m} x_{Ti}x_{Ri} + y_{Ti}y_{Ri}}\right) \tag{16.5}$$

Once again, in this equation *m* is the number of landmarks in the dataset.

There are a couple of things to note about using this equation. First, most software systems will express the arctangent of this ratio in terms of radians rather than degrees. If you want to know how many degrees you are rotating the R configuration through you'll need to convert the

radians to degrees. It's an easy conversion (see the *Palaeo-Math 101-2* spreadsheet for an example in MS-Excel).

Also, both Sneath (1967) and Rohlf and Slice (1990) recommend performing the calculation twice, once using the coordinate values determined by the scaling operation, and a second time after reflecting the one configuration (usually the *R* configuration) across the *x*-axis. This is a convention derived from generalized Procrustes analysis in which there is no necessary correspondence between individual points in the two datasets. It makes no sense in terms of geometric morphometrics as the reflection would result in mismatching landmark coordinates. Regardless, the fit achieved by the *Dalmanites* data after reflection is notably inferior to the fit achieved by the two datasets in their standard (= correct) configuration (see the *Palaeo-Math* 101-2 spreadsheet for details). The resulting Procrustes (GLS) fit between the two triangles is shown in Figure 4.

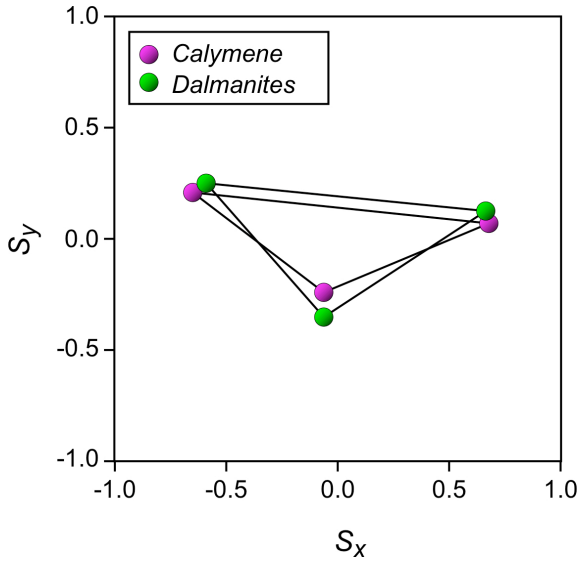

Figure 4. Trilobite pygidial landmark datasets after rigid rotation to minimize the sum of squared distances between corresponding landmarks. Note the space remains scaled to *RCS* units. The rotation angle specified by the GLS calculations was -7.20° (CCW).

Comparing Figure 4 to the results of the BSC alignment (Fig. 3 of MacLeod 2008) shows the effect of the distortion induced by baseline registration. By forcing all shape variation onto landmark 3 (posterior tip of the pygidia) shape distinctions in that region were grossly exaggerated. Specifically, the amount of pygidial elongation of the *Dalmanites* specimen relative to the *Calymene* specimen was reduced under Procrustes (GLS) alignment and a potentially important pygidial narrowing of the former relative to the latter, revealed. Of course, this narrowing of the *Dalmanites* pygidium was entirely obscured by the BSC analysis because landmarks 1 and 2 were used to define the baseline.

In a routine Procrustes (GLS) analysis the rotational alignment to a target configuration (usually the first specimen in a dataset) is the first stage of an iterative search for the optimal rotational alignment over all the shapes comprising the dataset. Once this first stage has been completed a mean configuration is calculated for all landmarks and this mean shape used as the target to which all other shapes are rotationally aligned in the second rotation cycle. Once this second cycle is complete the mean shape is re-estimated and another rotational alignment cycle conducted until the change in the fit achieved by this re-estimation procedure falls below a pre-set tolerance value. In practice, though, it is unusual for the estimation procedure to need to proceed beyond 2-3 rotational cycles.

Triangles are fun, but now let's see what Procrustes (GLS) superposition can tell us about our 18 trilobite cranidia. Recall last time we used six landmarks to assess shape variation over this structure (Fig. 5) with landmarks 1-4 representing the means of landmarks located on both sides of the mid-line after reflection of the right-side landmarks across the mid-line. This averaging operation removes left-right asymmetry from the landmark data. However, under the BSC approach we were only able to focus on the shape information provided by landmarks 1-4 as landmarks 5 and 6 were needed to define the BSC baseline.

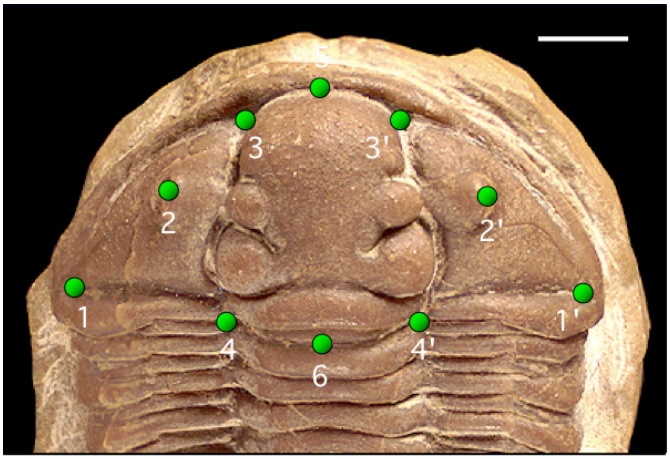

Figure 5. Landmarks used to quantify shape variation in the trilobite cranidium. Scale bar = 7.87 mm. 1: apex of the posterior lateral projection. 2: centroid of the eye location. 3: intersection of the glabellar margin with the posterior-lateral boundary of the pre-glabellar area. 4: intersection between the proximal posterior of the posterior lateral projection and the posterior lateral margin of the glabella. Landmark 5: anterior mid-line terminus. 6: posterior mid-line terminus. In the superposition procedure both left and right-side landmarks were used together to achieve and overall Procrustes (GLS) alignment. The right-side aligned landmarks were then reflected across the midline and averaged with their left-side counterparts.

Given the taxonomic diversity of this dataset, and given the broad discrepancies in cranidial shape suggested by the comparison of Bookstein shape coordinates (see MacLeod 2008, Fig. 9), the tightness and aspects of the form of the Procrustes (GLS) superposed landmark clusters, as seen in Figure 6, may come as something of a surprise.

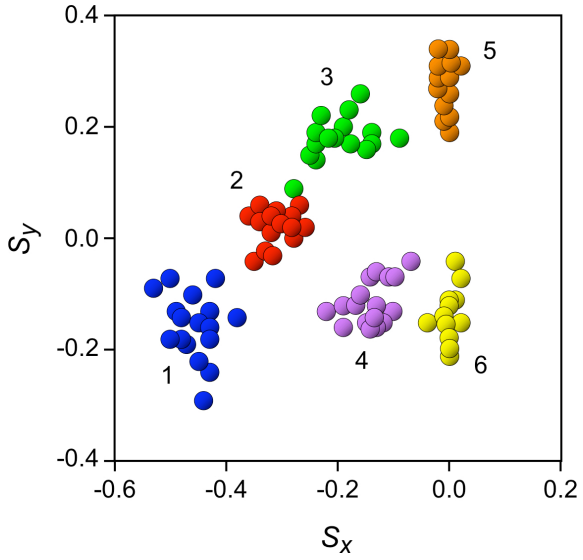

Figure 6. Results of a Procrustes (GLS) superposition of the six cranidial landmarks shown in Fig. 5. Points belonging to corresponding landmarks in each configuration set have been colour coded for clarity. These data represent mean positions from analogous landmarks on the right and left sides of the cranidia that have been reflected across the cranidial mid-line (landmarks 5 and 6). Note the well-constrained nature of all landmark clusters along with the relatively small number shape outliers. This is a very different picture of shape variation in these data than that suggested by the calculation of Bookstein shape coordinates (see MacLeod 2008, Fig. 9).

In addition to the improved resolution gained as a result of being able to include all landmarks in the assessment of shape variation, note that each landmark location exhibits approximately the same range of variation. Some clusters are a bit larger than the others (e.g., Landmark 1 vs.

Landmark 2), but all are remarkably similar.[2] This result stands in stark contrast to that obtained from the Bookstein shape coordinates (MacLeod 2008, Fig. 9) in which there was a marked tendency for landmarks located further away from the baseline to exhibit a greater degree of variation. This bias toward the artificial inducement of large amounts of variation in landmarks located distal to the baseline is related to the Bookstein method's transference of shape variation from the baseline landmarks. Indeed, the difference between Figure 6 of this essay and Figure 9 of the previous essay, constitutes a rather dramatic demonstration of the degree with which the BSC space is distorted relative to the Procrustes (GLS) shape coordinate space. But does this make a difference to the subsequent analysis of shape variation using these data? Let's use a PCA of the Procrustes (GLS) superposed coordinates to find out.

Table 2. Eigenvalues of PCA of GLS superposed coordinates.

Principal Component	Eigenvalue	Variance (%)	Cum. Variance (%)
1	0.00596	35.84	35.84
2	0.00452	27.18	63.02
3	0.00310	18.64	81.66
4	0.00118	7.10	88.76
5	0.00080	4.81	93.57
6	0.00045	2.71	96.27
7	0.00036	2.16	98.44
8	0.00026	1.56	100.00
9	-	-	-
10	-	-	-
11	-	-	-
12	-	-	-

The first thing to note is that, unlike the PCA analysis of other variable types, use of PCA to analyze GLS superposed shape coordinate data results in a lower than expected number of non-zero eigenvalues. In this example we might have expected to see a 12-axis PCA solution when, in point of fact, there are only 8 effectively non-zero eigenvalues.[3] This results from the various standardizations undertaken as part of the GLS superposition procedure. Two dimensions of variation are lost through standardization for the landmark configuration centroids, and another two as a result of the scaling and rotation standardizations. This loss of information will have implications for the statistical analysis of GLS superposed data that I'll discuss in future columns.

In addition to this you'll notice that the sequence of eigenvalue relative magnitudes (seen best in the Variance (%) and Cumulative Variance (%) columns of Table 2) are not as extreme as the values we've seen before. This is a consequence of removing positional, scaling and rotational sources of variation from the dataset and use of the mean shape as the final target for Procrustes (GLS) superposition.

Other than these qualitative differences, the interpretation of the eigenvector table of a PCA of Procrustes (GLS) superposed data is no different than interpretation of this table for any PCA analysis. For these data the first three components each account for more than 10 percent of the observed shape variation and first six component account to 95 percent of the total shape variation observed. For graphical simplicity we'll look at only the first three components in detail.

---

[2] Clusters of points assigned to landmarks 5 and 6 are strung out along the cranidial midline as a consequence of using the entire (left and right) landmark sets in the original GLS superposition, prior to left-right landmark reflection and averaging to achieve a consensus representation of inter-cranidial shape variation.

[3] The eigenvalues associated with axes 9-12 are not 0.00, but very small numbers (c. $< 10^{-8}$).

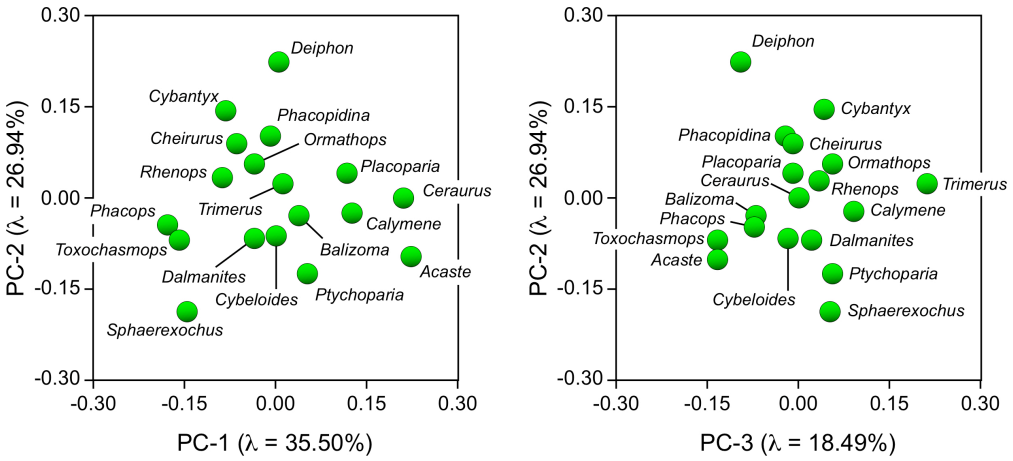

Figure 7. Scatter plots of cranidial GLS superposed landmark data in the space of the first three convariance-based principal components. See text for discussion.

Comparison of the Procrustes (GLS)-PCA scatterplots (Fig. 7) with the BSC-PCA scatterplots from the previous essay (MacLeod 2008, Fig. 8) is instructive. Whereas the overall range of shape variance has been reduced through use of Procrustes (GLS) superposition, shape relationships within the dataset are much more clearly resolved. To some extent this improved resolution results from the ability to sense shape variation at all landmarks as well as to the lack of systematic bias in the assignment of shape variation to landmarks based on their proximity to the BSC baseline. For this particular group of trilobites, whereas the broad distinctions between *Acaste*, *Calymene*, and *Ceraurus* with respect to *Toxochasmops* and *Phacops* both of which were identified by the previous BSC-PCA analysis as the most prominent distinctions within the dataset, were confirmed by the Procrustes (GLS) approach, *Trimerus* has now moved to a central position within the overall shape distribution. Along PC-2 and PC-3 the re-orderings are even greater. The group of taxa (incl. *Cybantyx*, *Cheirurus*, *Ormathops*, *Placopidina*, *Deiphon*, and *Rhenops*) that had previously shown a very strong shape similarity on both PC-1 and PC-2 axes has exploded in the Procrustes (GLS) shape space to occupy the entire region along the higher reaches of PC-2 and PC-3. This increase in shape variation makes similarity relations between this subset of forms much easier to assess and interpret.

Table 3. Procrustes (GLS) loadings for the first three covariance-based PC axes.

Shape Coords	PC-1	PC-2	PC-3
1x	0.318	-0.308	-0.148
1y	-0.593	-0.519	0.171
2x	0.166	0.096	-0.315
2y	0.087	0.036	-0.131
3x	-0.382	0.468	-0.390
3y	0.014	0.204	-0.504
4x	-0.079	0.276	0.340
4y	0.086	0.383	0.378
5x	-0.028	-0.053	-0.003
5y	0.438	-0.319	-0.185
6x	0.035	0.068	-0.003
6y	0.398	0.180	0.367

As we've seen before, a geometric interpretation of the PC space can be made via inspection of the PC axis loading coefficient table (Table 3). The PC-1 axis represents a shape change trend dominantly involving landmarks 1, 3, 5, and 6 (see Fig. 5 for landmark locations and definitions). Taking the signs of the loadings into account, landmark 1 moves laterally and anteriorly relative to the centroid along the positive portion of PC-1, effectively shortening the lateral aspect of the cranidia anterio-posteriorly and having the reverse effect along the negative portion of that axis. Landmarks 5 shifts anteriorly relative to other landmarks and landmark 6 shifts posteriorly, but

both move at a lower rate than the forward migration of landmark 1. Geometrically, this means the lateral portion of the cranidium migrates forward relative to the mid-line resulting in an overall sweeping of the lateral landmarks forward as one moves in positive direction along he PC-1 axis and backward as one moves in a negative direction. In addition to this, landmark 3 moves closer to the mid-line as the shape space location changes in a positive direction along PC-1 and further away from the mid-line as it changes in a negative direction. This interpretation is confirmed by inspecting the shape coordinate configurations for genera that scatter along the PC-1 axis (e.g., compare landmark distributions for *Rhenops* with *Ceraurus* in the *Palaeo-Math 101-2* spreadsheet).

The PC-2 axis represents a contrast between shape changes in the lateral margin of the cranidia (landmark 1) and in the glabella (landmarks 3 and 4). Here landmark 1 moves closer to the mid-line and forward along the positive portion of PC-2, reversing this trend along the negative portion. At the same time, the high and uniformly positive loadings on landmarks 3 and 4 indicate that the glabella expands outward from the centroid as as the shape space location changes in a positive direction along PC-2 with a differentially large lateral expansion in the anterior sector (landmark 3*x*) and a differentially large posterior-ward migration in the posterior sector (landmark 4*y*). In addition to this, the entire mid-line shifts backward relative to the other landmarks slightly, but at a lower rate than forward migration of the lateral landmarks (1*y*) and the expansion outward of the glabellar landmarks. This interpretation can be confirmed by inspecting the shape coordinate configurations for genera that scatter along the PC-2 axis (e.g., compare landmark distributions for *Balizoma* with *Deiphon* in the *Palaeo-Math 101-2* spreadsheet).

Finally, the PC-3 axis primarily represents a differential anterior contraction (landmarks 3*x* and 3*y*) and posterior expansion (landmarks 4*x*, 4*y*, and 6*y*) of the glabella along the positive portion of the PC-3 axis with this shape change trend reversing polarity along the negative portion. Accompanying this bulging out of the posterior glabella there is a pronounced relative migration of the lateral landmarks (1*x*, 1*y*) toward the mid-line and forward as signalled by the difference in the shape changes specified for landmarks 1, 3, 4, and 6. These shape trends are reversed in along the negative portion of the PC-3 axis and the overall interpretation confirmed by inspection for genera that scatter along the PC-3 axis (e.g., compare landmark distributions for *Balizoma* or *Toxochasmops* with *Trimerus* in the *Palaeo-Math 101-2* spreadsheet).

I'll have more to say about Procrustes (GLS) superposition in the next essay, which will deal with shape theory. That essay will explain, at long last, what the morphometric synthesis was all about and why the direct analysis of landmarks improves our ability to make interpretations of shape and shape change with confidence. But I don't want to leave you with the impression that the Procrustes (GLS) approach to superposition can solve all the interesting problems in comparative morphology. As a last brief, example, consider the following two forms (Fig. 8).

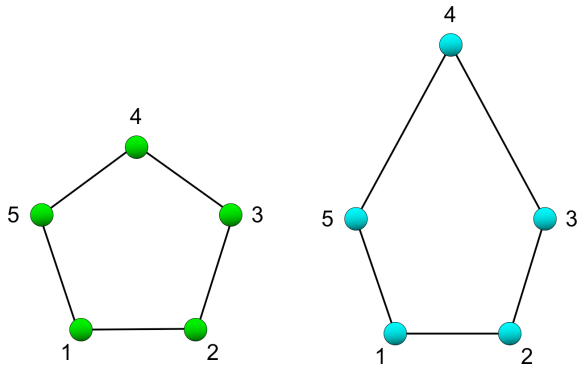

Figure 8. landmark configurations illustrating the 'Pinocchio Effect'.

Obviously the figure on the left is a pentagon with landmarks at the figure's vertices. The figure on the right is the same pentagon, but one I've deformed by increasing the height of the apical landmark (4). What will happen when we try the Procrustes (GLS) approach on these figures? Since we know there is absolutely no difference in the relative positions of landmarks 1, 2, 3, and 5, we'd like to see a superposition configuration that overlays these landmarks and

identifies landmark 4 as the odd one out. However when we apply the Procrustes (GLS) algorithm as shown in Figure 9.

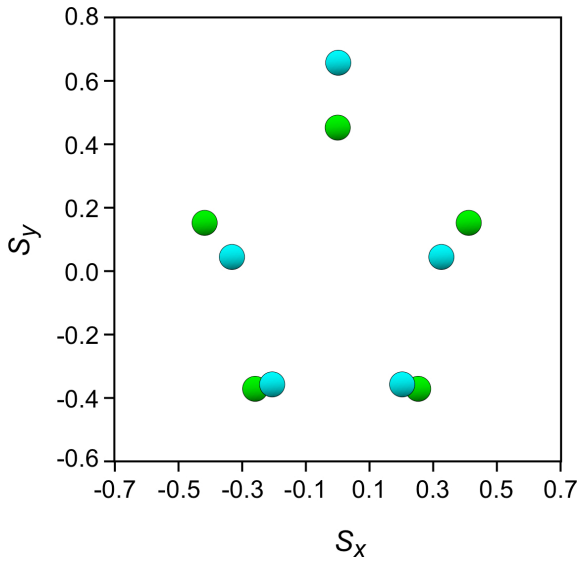

Figure 9. Procrustes (GLS) superposition of the landmark coordinates shown in Fig. 9 illustrating the 'Pinocchio Effect'.

As you can see (and as you probably already guessed), the Procrustes (GLS) algorithm will not handle this situation as we might like. In the jargon of morphometrics this is called the "Pinocchio Effect" after the wooden boy whose nose (but no other body part) grew every time he told a lie. If there is reason to believe a landmark dataset contains a Pinocchio Effect you may not want to use Procrustes (GLS) superposition as that algorithm will try to partition the overall shape variation over all landmarks once the effects of translation and scaling, have been removed. Of course, in this particular example the we could resolve the problem quite easily by opting to use Bookstein shape coordinates and selecting two landmarks from among the invariant set to define the baseline. For situations in which you suspect a Pinocchio Effect might exist, but you have no idea where the invariant parts of the form are (and don't feel you have time to conduct any exploratory experiments), there is an alternative form of Procrustes superposition—Resistant Fit Theta-Rho Analysis (RFTRA, see Siegel and Benson, 1982 for the original description or Rohlf and Slice, 1990 for a more compact, algorithm). The Procrustes (RFTRA) method uses an iterative approach to find the relatively invariant landmarks and arrive at a solution that (1) minimizes positional differences between subsets of landmark locations that are similar in position and (2) maximizes differences between subsets of landmarks whose positions differ. This having been said, Procrustes (RFTRA) usually offers only a partial solution that minimizes the overall Pinocchio Effect, but rarely eliminates it entirely.

In terms of software, there are a reasonable number of programs available for implementing a Procrustes (GLS) superposition. Jim Rohlf's Stony Brook (SB) Morphometrics web site (http://life.bio.sunysb.edu/morph/) lists several including continuously updated versions of Jim's own software. I've implemented the basic steps in the Sneath version of GLS superposition in this essay's *Palaeo-Math 101-2* spreadsheet and have developed *Mathematica* routines for performing either Sneath-style of Gower-style Procrustes (GLS) variants. Other, commercial software packages also include Procrustes analysis options and not just in statistical and/or numerical analysis software. Indeed, Procrustes algorithms also figure prominently in many 3D data manipulation packages under the guise of registration tools. As usual, it's best to check the user's guide or the software's technical support guru for advice on exactly what algorithm has been implemented and what range of options have been designed into any software package you are considering for use on your data.

Norman MacLeod
Palaeontology Department, The Natural History Museum
N.MacLeod@nhm.ac.uk

REFERENCES

BENSON, R. H. 1967. *Muscle-scar patterns of Pleistocene (Kansan) ostracodes*. In C. Teichert and E. L. Yochelson, eds. *Essays in paleontology and stratigraphy, Department of Geology, University of Kansas Special Publication No. 2*. Department of Geology, University of Kansas Special Publication No. 2, Lawrence, Kansas. 211–214 pp.

GOWER, J. C. 1971. *Statistical methods of comparing different multivariate analyses of the same data*. In F. R. Hodson, D. G. Kendall, and P. Tautu, eds. *Mathematics in the archaeological and historical sciences*. Edinburgh, Edinburgh University Press. 138–149 pp.

GOWER, J. C. and DIJKSTERHUIS, G. B. 2004. *Procrustes problems*. Oxford University Press, Oxford. 248 pp.

KIM, K., SHEETS, D., HANEY, R. A. and MITCHELL, J. T. 2002. Morphometric analysis of ontogeny and allometry of the Middle Ordovician trilobite *Triarthrus becki*. *Paleobiology*, 28(364–377).

MacLEOD, N. 2005. Regression 4: Going Multivariate. *The Palaeontological Association Newsletter*, 58, 44–53.

MacLEOD, N. 2008. Size and shape coordinates. *Palaeontological Association Newsletter*, 69, 26–36.

MARDIA, K. V. and DRYDEN, I. L. 1989. Shape distributions for landmark data. *Advances in Applied Probability*, 21, 742–755.

ROHLF, F. J. and SLICE, D. 1990. Extensions of the Procrustes method for optimal superposition of landmarks. *Systematic Zoology*, 39, 40–59.

SIEGEL, A. F. and BENSON, R. H. 1982. A robust comparison of biological shapes. *Biometrics*, 38, 341–350.

SNEATH, P. H. A. 1967. Trend surface analysis of transformation grids. *Journal of Zoology*, 151, 65–122.

WEBSTER, M., H. SHEETS, D., and HUGHES, N. C. 2001. *Allometric patterning in trilobite ontogeny: testing for heterochrony in Nephrolemellus*. In M. L. Zelditch, ed. *Beyond heterochrony*. John Wiley & Sons, New York. 105–142 pp.

ZELDITCH, M. L., SWIDERSKI, D. L., SHEETS, H. D. and FINK, W. L. 2004. *Geometric morphometrics for biologists: a primer*. Elsevier/Academic Press, Amsterdam. 443 pp.

Don’t forget the *Palaeo-math 101-2* web page, now at a new home at:
http://www.palass.org/modules.php?name=palaeo_math&page=1